

RESEARCH PAPER

## Investigation of Copper/Sodium Alendronate Drug Doped TiO<sub>2</sub> Nanoparticle Array on Ti as a Hybrid Material for Implant Application

Neda Aryan<sup>1</sup>, Ali Benvidi<sup>1\*</sup>, Mohsen Behpour<sup>2</sup>, Fereshteh Jookar Kashi<sup>3</sup>, Mostafa Azimzadeh<sup>4</sup>, and Hamid R. Zare<sup>1</sup>

<sup>1</sup> Department of Chemistry, Faculty of Science, Yazd University, Yazd 8915818411, Iran

<sup>2</sup> Department of Analytical Chemistry, Faculty of Chemistry, University of Kashan, Kashan, Iran

<sup>3</sup> Department of Cell and Molecular Biology, Faculty of Chemistry, University of Kashan, Kashan, Iran

<sup>4</sup> Department of Advanced Medical Sciences and Technologies, School of Paramedicine, Shahid Sadoughi University of Medical Sciences, Yazd, Iran

### ARTICLE INFO

#### Article History:

Received 12 December 2024

Accepted 21 March 2024

Published 01 April 2024

#### Keywords:

Corrosion

Drug release

Implant

Nanoparticles

Osteoporosis

Titanium dioxide

### ABSTRACT

Titanium is the optimal biomaterial for orthopedic and dental applications. Due to its biocompatibility and superior mechanical properties, it is more suitable for implant applications than other metals. However, due to its bio-inertness, the surface of titanium must be modified for human bone tissue. Various techniques can be used to construct titanium dioxide (TiO<sub>2</sub>) nanoparticles (TNPs), but anodizing is the most often used because of its portability and low cost. Due to the high similarity of hydroxyapatite to the mineral components of bone and dentin, metal implants are coated with bone-conducting biomaterials such as hydroxyapatite (HA) to enable better bone bonding. In this study, copper and chitosan were used because of their excellent antimicrobial properties. Electrochemical impedance tests show that an HA/Cu/Drug/chitosan (Chit) coating has a polarization resistance of 300,000 Ω because the copper coating on the titanium dioxide nanoparticle (TNP) increases corrosion resistance. A potentiodynamic polarization test shows that the current of corrosion of the HA/Cu/Drug/chitosan sample is  $2.1719 \times 10^{-6}$  A. The antibacterial activity of the HA/Drug, HA/Drug/Chit, and HA/Cu/Drug/Chit coatings was evaluated in vitro against *Staphylococcus aureus* ATCC 29737, and it is found that the HA/Cu/Drug/Chit coating presents high antibacterial activity due to the presence of copper and chitosan. Its optical density is 0.78, which is lower than that of all the other samples. Cell viability is highest for the TNP samples containing chitosan. Regarding the TNP sample containing HA/Drug (99.4%), it is observed that the percentage of cell viability is higher than that of the TNP sample containing HA/Cu/Drug (97.54%) due to the toxicity of copper. This study shows that the modification of the titanium implants can be used to control drug release and enhance corrosion resistance, antibacterial properties, and cell viability.

### How to cite this article

Aryan N., Benvidi A., Behpour M., Jookar Kashi F., Azimzadeh M., Zare H. Investigation of Copper/Sodium Alendronate Drug Doped TiO<sub>2</sub> Nanoparticle Array on Ti as a Hybrid Material for Implant Application. *J Nanostruct*, 2024; 14(2):437-451. DOI: 10.22052/JNS.2024.02.007

\* Corresponding Author Email: [abenvidi@yazd.ac.ir](mailto:abenvidi@yazd.ac.ir)



## INTRODUCTION

In recent years, the successful application of orthopedic implants to related diseases such as osteomyelitis and osteoporosis has been a major concern [1]. Hip replacements, which involve the replacement of a problematic human hip joint with an artificial hip joint, are among the most successful orthopedic surgeries [2]. A hip replacement is a medical procedure that is performed to physically replace a damaged human hip joint with a hip prosthesis [3].

Metal ions are produced from the wear of particles in metal-on-metal bearings that circulate in the body and cause local inflammation [4]. Abraded metal particles can spread through the lymphatic system to regions far from the implant and accumulate in the liver, spleen, lymph nodes, and bone marrow [5]. In the design of porous implants, permeability is essential as a function of cell migration and bone tissue regeneration. In this study, a porous implant was created according to the morphological indicators of cancellous bone (including porosity, specific surface area, thickness, and torsion) [6]. However, active implant users with longer life expectancies still undergo reoperation due to implant failure [7]. Efforts made to prevent the failure of implants must further evaluate the selection of metal materials used for implants [8]. In addition, when an implant is used to replace lost tissue, it undergoes a complex process, especially for the degradation mechanism. This degradation mechanism is one of the most common reasons for failure; therefore, the use of a material that is biocompatible in terms of its biomechanical properties is optimal when selecting an implant [9]. Several metal materials can be used in implants, including cobalt chromium molybdenum (CoCrMo), stainless steel 316 L (SS 316 L), and titanium alloy [10]. These metals are widely used in the field of orthopedics in both temporary and permanent equipment [11]. Titanium (Ti) and its alloys are widely used in the manufacture of implants. The biocompatibility of Ti and its alloys is a result of the formation of a layer of titanium oxide (TiO<sub>2</sub>) on the surface of the implant. This passive oxide layer provides high stability, low chemical wear, permeability, and corrosion resistance in biological environments [12].

The corrosion of the metal implants in the human body due to the introduction of unwanted ions can affect biocompatibility and mechanical integration and cause adverse biological reactions

[13]. To ensure of the long-term stability of orthopedic implants, effective primary and secondary stabilization is required. Secondary stabilization supports the long-term stabilization of the implant and is often achieved through bone growth in a porous coating on the implant [14]. Effective primary stabilization is required for successful secondary stabilization [15–19]. Electrochemical anodizing is a commonly used method for the formation of pores/nanotubes on the surfaces of titanium metal. Numerous studies have reported that titanium surfaces with titanium dioxide nanoparticles (TNP) offer positive effects such as bone fusion, cell differentiation, and antimicrobial properties [20]. TNPs fabricated through electrochemical anodization have attracted a great deal of attention in biomedical applications due to their unique topography, low cytotoxicity, and low elastic modulus [21]. To meet patient and market needs, implants are developed using materials that ensure biocompatibility, strength, and appropriate weight [22] and that have features such as excellent hardness, strong wear resistance, a low friction coefficient, and superior toughness [23]. In addition to their proven biocompatibility, TNPs have sufficient bioactivity and enhanced cellular functions, enabling significant drug loading and the achievement of optimal release kinetics [24, 25]. Titanium dioxide is widely used in many other applications, ranging from self-cleaning surfaces to electronics, energy, and biotechnology [26]. These features constitute the characteristics of an ideal implant modification technology that can address the most common bone implant challenges and enable local drug delivery. The hollow structure of TNPs can be used as an alternative to orthopedics. It can also be used as an orthopedic drug carrier to aid topical therapy, improve the bioavailability of drugs, and reduce side effects [27–34]. Therefore, TNPs are increasingly attracting the attention of biomaterials scientists for using these materials as carriers of drugs and various species such as trace elements, growth factors, etc. [35].

The metal element copper has shown strong antibacterial behavior against a wide range of microbes, including resistant bacterial strains, and is one of the essential trace elements. In addition, it is capable of increasing the cellular compatibility of implant surfaces [36]. Several studies have reported that copper in hydroxyapatite coatings has beneficial effects on bone metabolism and

prevents bacterial adhesions [37].

The application of a hydroxyapatite bioceramic coating on biomedical metal substrates can significantly increase their mechanical strength for various applications [38]. Hydroxyapatite is one of the main components of bone, which is a derivative of calcium phosphate crystals and is situated between collagen fibers [39].

Chitosan has biocompatibility and antibacterial activity. The amino groups present in its structure affect killing bacteria. The mechanism of chitosan's antibacterial activity is that positively charged amines in chitosan attract the negatively charged bacterial cell wall and cause a disruption in the cell membrane [40].

The HA/Cu/Drug/Chit coating has unique properties for drug-eluting stents (DESs). A DES is designed to prevent in-stent restenosis by inhibiting smooth muscle cell proliferation. Drugs can be combined with polymers or minerals, or applied directly into the stent surfaces, slowly releasing the drug at the site [41]. The deposition of drugs on titanium-dioxide-coated implants and the development of drug-eluting implants seem to be effective strategies to reduce the corrosion rate and increase it post-infection [42].

In this research, titanium sheets were converted into TNP by the electrochemical anodization method. Hydroxyapatite and copper (with different concentrations) were deposited on the TNP's surface by chronopotentiometry. Sodium alendronate was coated onto the TNPs using the immersion method. Then, chitosan was coated onto the TNPs using the immersion method. Finally, after placing the coated TNP in the phosphate buffer solution, its absorption value was investigated on different days using a spectrophotometer. The released drug was evaluated using the drug calibration curve and the measured absorption values. The number of released copper ions in the phosphate buffer was also determined using a flame atomic absorption spectrometer. The conversion of metallic titanium into titanium dioxide creates pores and nanotubes, which causes the absorption and trapping of compounds such as hydroxyapatite, copper, drugs, and chitosan. In addition, the release rate is controlled. The novelty of the work is using titanium dioxide instead of titanium in these cases. The titanium sheet is converted to titanium dioxide by electrochemical anodization, and SEM analysis shows the growth of nanoparticles on the titanium

surface. Therefore, the synthesis of nanoparticles was done in this way. Hydroxyapatite and copper coating was used on the surface of TNP and the amount of release of copper ion and sodium alendronate drug was investigated.

## MATERIALS AND METHODS

### Characterization of Materials

The raw material of 99.5% purity Ti foil was purchased from the Nazari Company (Tehran, Iran). Chitosan was bought from the Sigma Chemical Company (St. Louis, MO, USA). The active ingredient of sodium alendronate was purchased from the Iran Daru Parseh Company (Tehran, Iran). *Staphylococcus aureus* ATCC 29737 was purchased from the microbial collection of the Scientific and Industrial Research Organization of Iran (Tehran, Iran). Other materials were purchased from the Merck Company (Darmstadt, Germany).

X-ray diffraction (XRD) patterns were recorded by a Philips X'Pert Pro X-ray diffractometer using Ni-filtered Cu K $\alpha$  radiation at a scan range of  $10 < 2\theta < 80$ . The morphology of the films that were obtained at 17.5 kV performance was determined by field emission scanning electron microscopy (FESEM, Zeiss, and Gaithersburg, Germany). FESEM images with energy-dispersive X-ray spectroscopy were obtained on an LEO-1455VP. The energy dispersive spectrometry (EDX) analysis was studied by an XL30 Philips microscope. Electrochemical impedance spectroscopy and potentiodynamic polarization experiments were performed by an Atolab potentiostat-galvanostat PGSTAT 35 (Eco Chemie, Utrecht, and The Netherlands). The polarization test was performed at the scanning speed of 0.001 v/s, and the electrochemical impedance was performed in the frequency range of 0.1 Hz to 100 kHz. The UV-Vis absorption spectra of sodium alendronate drug in buffer were recorded using a double-beam spectrophotometer (PerkinElmer (Markham, ON, Canada) Lambda 25 UV-Vis Spectrophotometer) in Suprasil quartz cells of 1 cm optical path length, and the absorbance of the samples was measured in the wavelength of 254 nm. The electrodeposition method was performed for coating TNP with HA and Cu with a SAMA 500 model potentiostat-galvanostat. The amounts of Cu deposited on the TNP and released in the buffer were determined by a PerkinElmer model atomic absorption spectrophotometer. The surface resistance value of TNP was determined by the FPP-SN-555 model four-point probe.

**TNP Formation and Measuring the Surface Resistance of TNP**

Anodizing of titanium foil was performed to convert titanium foil into titanium dioxide in an electrolyte solution consisting of 0.3 g of ammonium fluoride, 3 mL of deionized water, and ethylene glycol (97 mL). Anodization was performed at a voltage of 60 V for 45 min in a two-electrode system consisting of titanium (working electrode) and platinum sheets (counter electrode). Finally, titanium dioxide was placed in the furnace at 450 °C for 1 h.

The resistance of the surface amount of TNP was investigated with a four-point probe device.

**Cu-HA Formation on TNP**

TNPs were coated with hydroxyapatite and copper by the electrodeposition method. Electrodeposition was performed with a three-

electrode system in the workstation. Titanium foil, platinum, and Ag/AgCl (KCl 3.0 M) were selected as the working, the counter, and the reference electrodes, respectively. Calcium nitrate with a concentration of 0.042 M, copper nitrate with different concentrations containing 0.001, 0.002, and 0.003 M, and ammonium dihydrogen phosphate with a concentration of 0.25 M in a volume of 50 mL at a pH of 4.5 were selected as the electrolyte solution. Then, the experiment was performed by chronopotentiometry with a constant current intensity of 1 mA for 25 min at 65 °C.

**Preparation of Phosphate Buffered Saline (PBS)**

First, for PBS preparation, 2.0 g of NaCl, 0.05 g of KCl, 0.36 g of Na<sub>2</sub>HPO<sub>4</sub>, and 0.06 g of KH<sub>2</sub>PO<sub>4</sub> were placed in 200 mL of deionized water. The solution temperature was adjusted to 37 °C with a

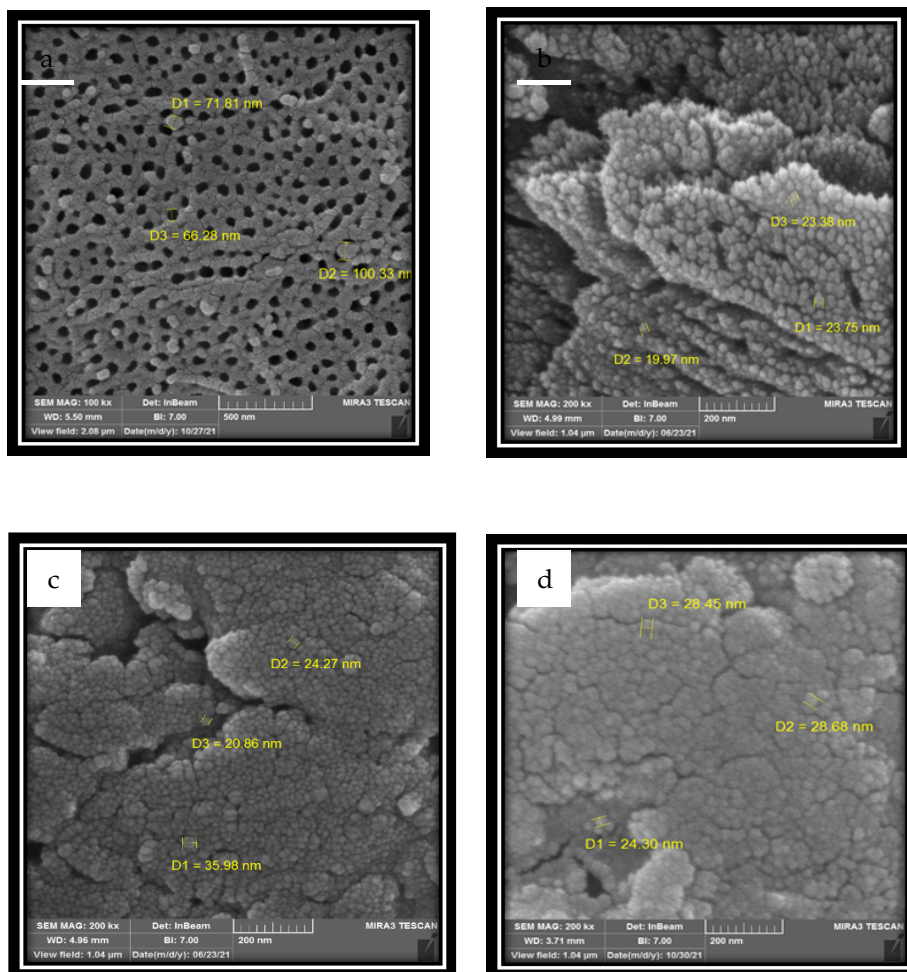


Fig. 1. FESEM images of (a) TNP (b) TNP/HA/Drug (c) TNP/HA/Drug/Chit (d) TNP/HA/Cu/Drug/Chit.

deionized water bath, and the pH was adjusted to 7.4 with a HCl solution and diluted to 250 mL with deionized water.

*Loading of Drug and Chitosan into TNP*

A drug concentration was dissolved in PBS (0.08 g of drug in 4 mL PBS). The coating was done by immersion of the TNP for 3 min repeated 20 times, and finally, 1% chitosan was coated onto the nanoparticles by the same method.

*Studies of Drug and Copper Ion Release*

The nanoparticles coated with HA/Drug, HA/Drug/Chit, and HA/Cu/Drug/Chit were placed in PBS at 37 °C. On the first, second, fourth, eighth, and sixteenth days, the PBS was replaced with a fresh PBS. Finally, the buffer samples were collected and the amount of the released drug was recorded using a UV–Visible device and a calibration curve was plotted. The equation of the calibration curve of alendronate sodium drug is equal to:

$$Y = 0.5286x - 0.0018$$

Using atomic absorption, the amount of the released Cu was investigated for the HA/Cu/Drug/Chit sample.

*Electrochemical Study*

Impedance and polarization data were

collected using a standard three-electrode system (working, counter, and reference electrodes) and an electrochemical workstation. Open circuit potential was performed by immersing the modified, counter, and reference electrodes in PBS. The obtained data were expressed in impedance and Tafel plots from which corrosion current and polarization resistance were obtained.

*Antimicrobial Properties and Cell Viability Assay*

To evaluate the antimicrobial properties of TNP, TNP/HA/Drug, TNP/HA/Drug/Chit, and TNP/HA/Cu/Drug/Chit samples after inoculation of *S. aureus* ATCC 29737 in the nutrient broth medium, the samples were incubated at 37 °C to reach turbidity of half a McFarland. In total, 20 mL of the suspension and four samples of TNP/HA/Drug, TNP/HA/Drug/Chit, and TNP/HA/Cu/Drug/Chit were placed inside four Erlenmeyer flasks. The fifth Erlenmeyer flask contained only suspension; no sample was placed inside, and this was considered the control sample. The Erlenmeyer flasks were then placed in a 37 °C shaker incubator for 24 h. Optical density (OD) was recorded to measure the number of microorganisms after 24 h with an ultraviolet spectrophotometer at 600 nm. To examine the adhesion of *S. aureus* to the implant, after removing the samples from the suspension after 24 h, they were washed with physiological saline to separate the bacteria from the non-adherents. After placing the samples in a

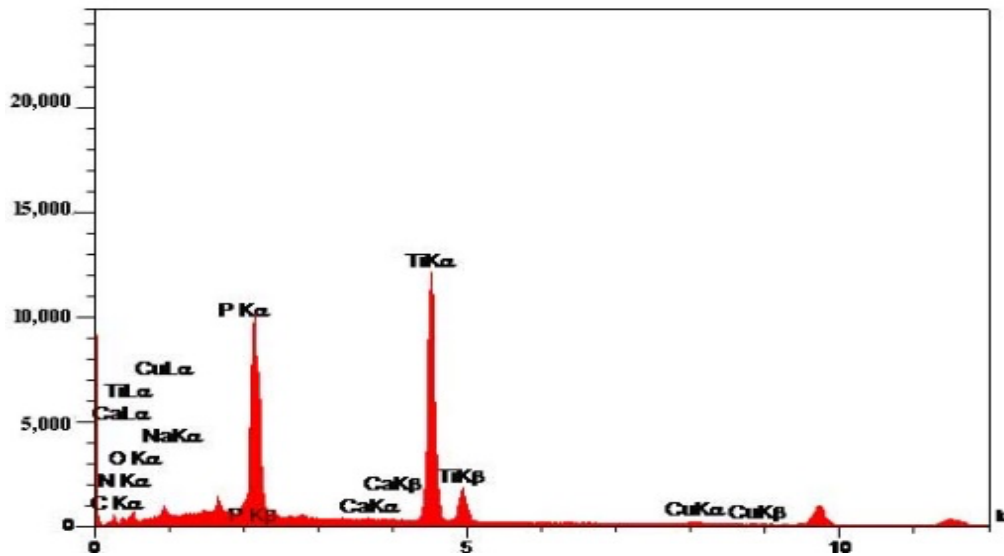


Fig. 2. EDX images of TNP/HA/Cu/Drug/Chit sample.

test tube containing 10 mL of physiological serum, they were placed in an ultrasonic bath for 5 min to remove bacteria adhering to the implant surface. Then, 10  $\mu$ L from bacterial cells isolated from the implant surface was inoculated on each of four plates containing nutrient agar medium and placed in an incubator at 37  $^{\circ}$ C for 24 h.

Cell viability analysis was performed by the US

Food and Drug Administration. Minor changes are described in detail in the literature [43].

## RESULTS AND DISCUSSION

### *Characterization of TNP Coating and Measuring the TNP Resistance of Surface*

The structure and morphology of the TNPs and the modified TNPs were studied by FESEM

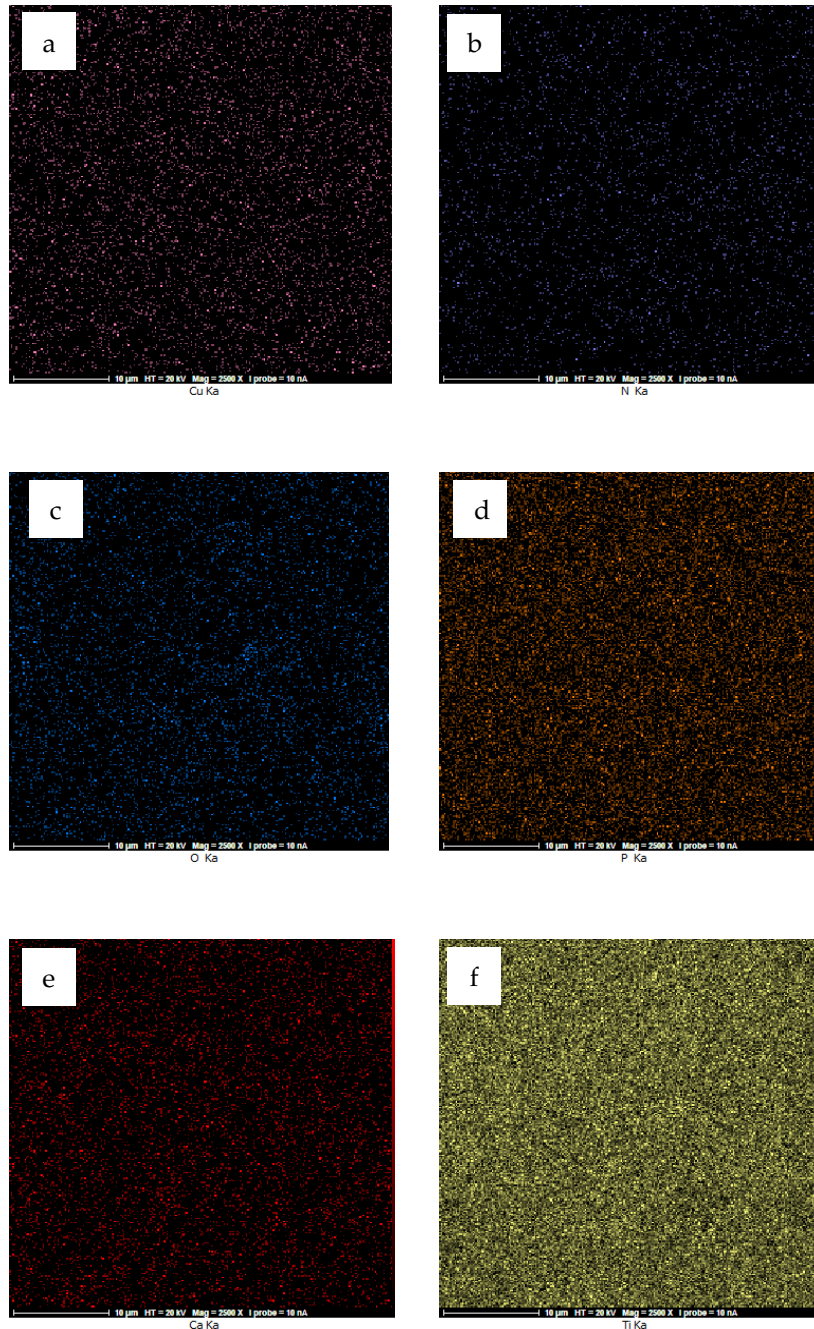


Fig. 3. EDX mapping spectrum of (a) Cu (b) N (c) O (d) P (e) Ca (f) Ti.

images. Fig. 1a shows the TNPs. The nanoparticles are uniformly distributed throughout the titanium substrate. Fig. 1b shows the TNPs modified with the drug and hydroxyapatite. A uniform distribution of hydroxyapatite is observed at the titanium dioxide nanoparticle level. This observation is related to the good correlation between hydroxyapatite and the drug. Fig. 1c shows the TNPs modified with chitosan in addition to hydroxyapatite and the drug. The pores are covered by the chitosan polymer layer, and the thickness of the nanoparticles has increased. Fig. 1d shows the TNPs modified with hydroxyapatite, copper, the drug, and chitosan. With the presence of copper, the particles are more uniformly placed on the surface of the TNP. Copper-ion-substituted hydroxyapatite was coated on TNP's surfaces. Fig. 1a shows that the pores are empty. When we load materials into nanoparticles, the materials enter the pores (Fig. 1b–d). These images confirm the

presence of materials inside the TNP. The average particle diameter is about 27.03 nanometers. Fig. 2 shows the EDX image of the TNP coated with HA/Cu/Drug/Chit. The structure of hydroxyapatite, copper nitrate, titanium dioxide, and chitosan contains Ca, N, O, P, Ti, Na, C, and Cu elements. Therefore, Fig. 2 shows these elements present on the TNP's surface. Fig. 3 shows the presence of these elements on the TNP's surface. Fig. 4 shows the XRD of a TNP coated with an HA/Cu/Drug/Chit sample. The JCPDS card number for copper nitrate is 01-074-2372, the JCPDS card number for titanium dioxide in the anatase phase is 01-083-2243, and the JCPDS card number for hydroxyapatite is 00-001-1008. The 2θ of 25.5°, 48.1° is related to titanium dioxide in the anatase phase. The 2θ of 53.3° is related to hydroxyapatite, and the diffraction peaks with 2θ of 35.4°, 40.44°, 54.3°, 63.3°, and 71° indicate copper in the sample. The value of the surface resistance of the TNPs

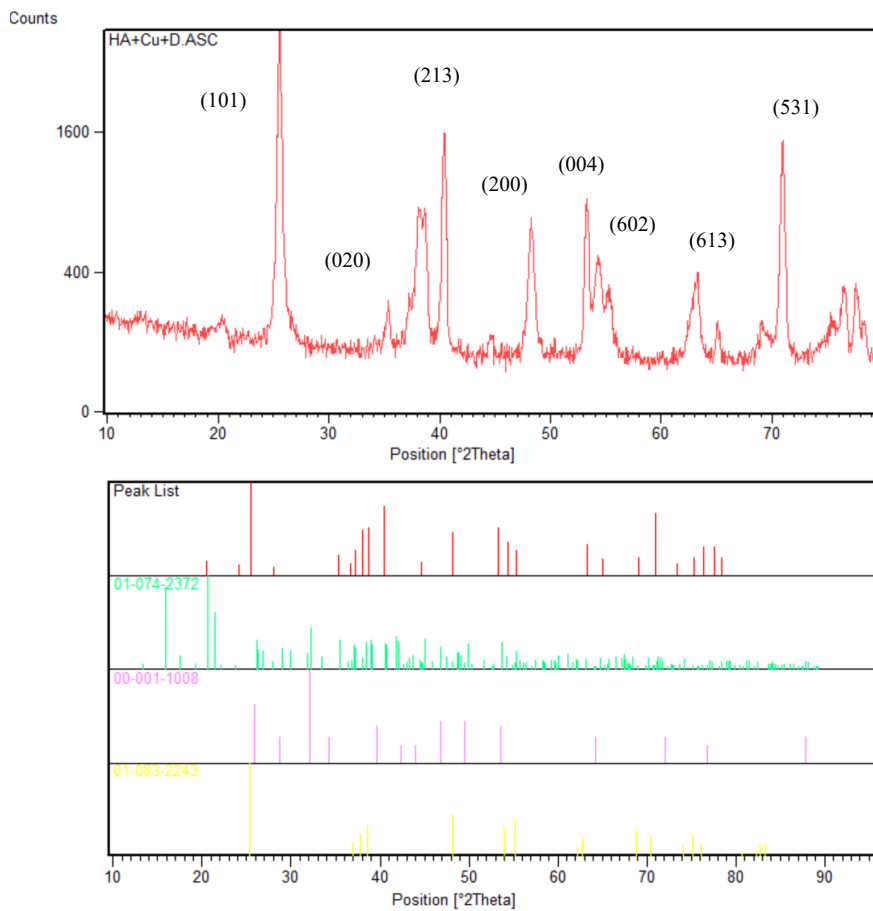


Fig. 4. Diffraction of X-ray of TNP/HA/Cu/Drug/Chit.

was investigated with a four-point probe device. The conductivity of the TNPs was confirmed by measuring the resistance of the surface value of the TNPs (0.071 Ω/square).

Fig. 5 shows the optical density for the samples of TNP, TNP/HA/Drug, TNP/HA/Drug/Chit, and TNP/HA/Cu/Drug/Chit after 24 h. The optical density of the TNPs coated with HA/Cu/Drug/Chit is lower than that of the TNPs coated with HA/Drug/Chit because the copper element may be a promising antibacterial agent, as one of the transition metal elements released from TNPs, which may have a lethal effect by inhibiting the adhesion of bacteria. The optical density of TNPs coated with HA/Drug/Chit is lower than that of TNPs coated with HA/Drug. This is due to the presence of chitosan, which has antibacterial properties. The optical density of the TNP sample is the highest because of the lack of layering. The optical density of TNPs coated with HA/Cu/Drug/Chit is lower than all of the samples due to the simultaneous presence of copper and chitosan, increased antibacterial effect, and lower optical density value.

Fig. 6 shows the adhesion of bacteria for TNP, TNP/HA/Drug, TNP/HA/Drug/Chit, and TNP/HA/Cu/Drug/Chit samples on the implant surface. In the sample of a TNP coated with HA/Cu/Drug/Chit, its bacterial adhesion is lower than that of a TNP coated with HA/Drug/Chit because the copper element may be an up-and-coming antibacterial

agent as one of the transition metal elements released from the TNP, which may have a lethal effect by inhibiting the adhesion of bacteria. The sample of TNP coated with HA/Drug/Chit has lower bacterial adhesion than that of TNPs coated with HA/Drug. This is due to the presence of chitosan, which has antibacterial properties. The TNP sample has the highest bacterial adhesion because of the lack of layering. The sample of TNPs coated with HA/Cu/Drug/Chit has lower bacterial adhesion than all samples because of the simultaneous presence of copper and chitosan, which means that the antibacterial properties are increased.

#### Electrochemical Studies

Polarization experiments and electrochemical impedance spectroscopy were performed to investigate the electrochemical behavior of the samples. Fig. 7 shows the polarization curves for TNP, TNP/HA/Drug, TNP/HA/Drug/Chit, and TNP/HA/Cu/Drug/Chit samples. In the sample of TNPs coated with HA/Cu/Drug/Chit, the current corrosion rate is lower than the sample of TNPs coated with HA/Drug/Chit due to the presence of copper, the increased number of layers, and the prevention of PBS penetrating the surface of the implant. The sample of TNPs coated with HA/Drug/Chit has a lower corrosion current rate than those coated with HA/Drug. Since the chitosan polymer molecules interact with the surface of titanium

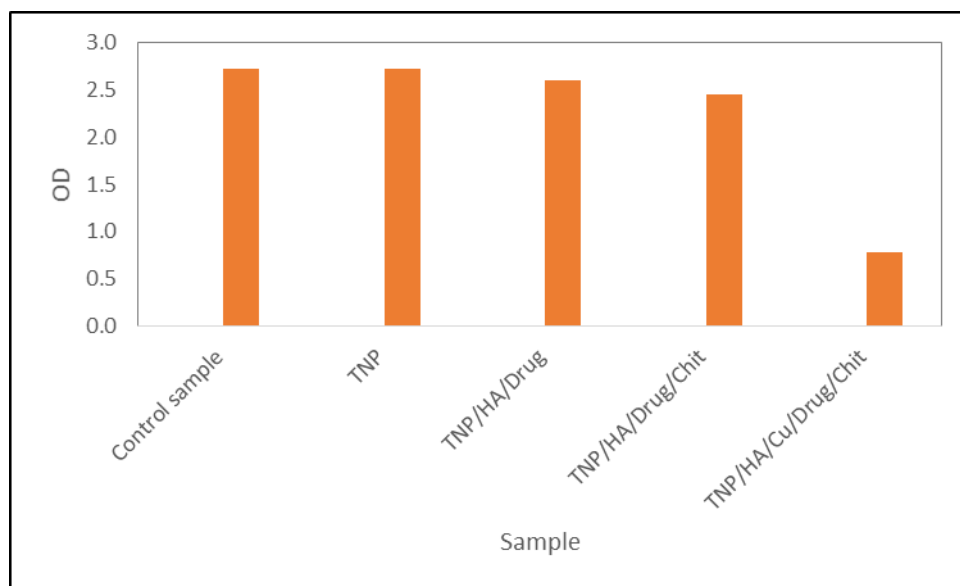


Fig. 5. Optical density of TNP, TNP/HA/Drug, TNP/HA/Drug/Chit, and TNP/HA/Cu/Drug/Chit samples after 24 h.

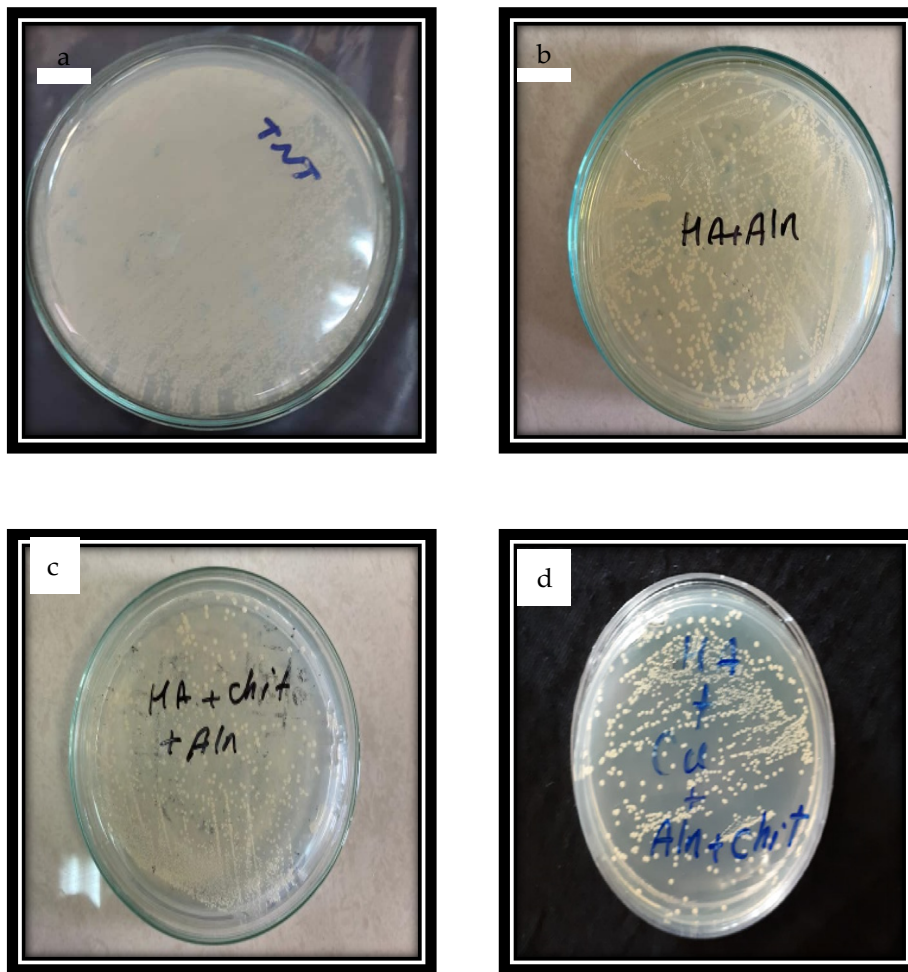


Fig. 6. The bacterial adhesion of (a) TNP (b) TNP/HA/Drug (c) TNP/HA/Drug/Chit (d) TNP/HA/Cu/Drug/Chit samples.

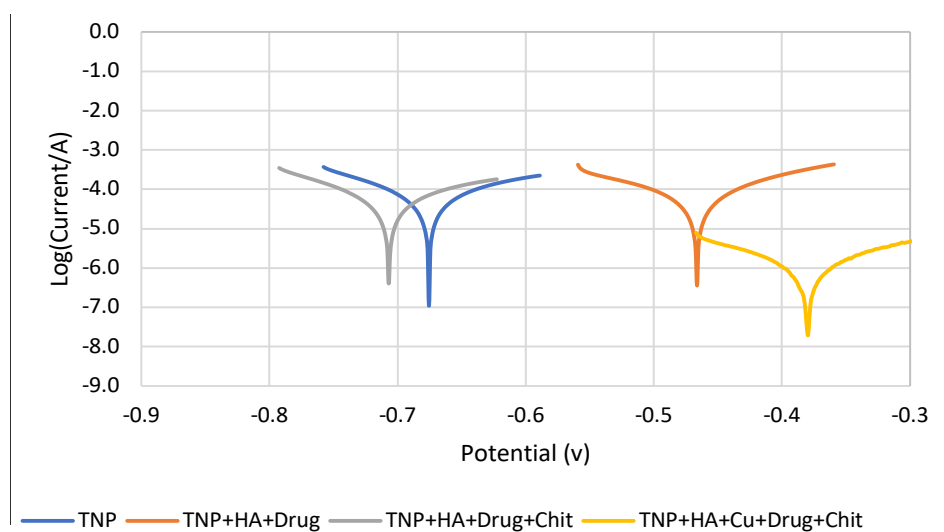


Fig. 7. Polarization curve of TNP, TNP/HA/Drug, TNP/HA/Drug/Chit, and TNP/HA/Cu/Drug/Chit samples.

dioxide by van der Waals forces, it increases the corrosion resistance of the TNP by separating the surface of the implant from the environment and preventing the contact of corrosive ions with it. Currently, the corrosion of the TNP sample is higher than all of the samples due to the lack of coating. Current corrosion values are shown in Table 1.

Fig. 8 shows the electrochemical impedance diagram of the different modified electrodes. The sample of TNPs coated with HA/Cu/Drug/Chit has a larger diameter of the capacitor ring than the sample of TNPs coated with HA/Drug/Chit due to the presence of copper, the increased number of layers, and the prevention of PBS penetrating the surface of the implant, so the polarization resistance is higher. The diameter of the capacitor ring of the TNPs coated with HA/Drug/Chit is

greater than that of the TNPs coated with HA/ Drug. Since the chitosan polymer molecules interact with the titanium dioxide surface with van der Waals forces, it increases the polarization resistance by separating the implant surface from the environment and preventing the contact of corrosive ions. The polarization resistance of the TNP sample is lower than all of the samples due to the lack of coating. After processing the impedance test results using the equivalent circuit, the polarization resistance obtained for the samples is shown in Fig. 9. The equivalent circuit for all samples is R<sub>1</sub>CPER<sub>2</sub>, where R<sub>1</sub> is the solution resistance, R<sub>2</sub> is the polarization resistance, and CPE is the coating capacity. R<sub>s</sub> and CPE values for the TNP sample are equal to 38.430 Ω and 0.634, respectively. R<sub>s</sub> and CPE values for HA/Cu/Drug/Chit sample are equal to 63.630 Ω, and 0.659,

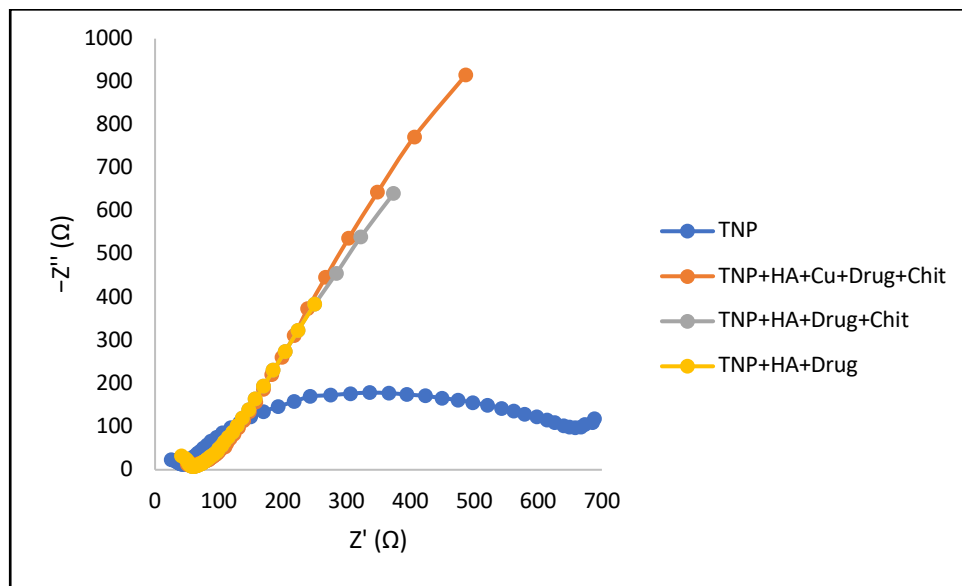


Fig. 8. Electrochemical impedance spectroscopy of TNP, TNP/HA/Drug, TNP/HA/Drug/Chit, and TNP/HA/Cu/Drug/Chit samples.

Table 1. Parameters extracted from the Tafel diagram for TNP, TNP/HA/Drug, TNP/HA/Drug/Chit, and TNP/HA/Cu/Drug/Chit samples.

Sample	TNP/HA/Cu/Drug/Chit	TNP/HA/ Drug/Chit	TNP/HA/ Drug	TNP
$j_{corr}$ (μA/cm <sup>2</sup> )	2.17	123.00	161.00	176.00
$E_{corr}$ (V)	-0.380	-0.706	-0.465	-0.676
BetaA (V/dec)	0.140	0.309	0.211	0.370
BetaC (V/dec)	0.324	0.193	0.311	0.231
$R_p$ (Ω)	19195.0	416.4	349.9	339.2

respectively.

The polarization resistance values for all of the electrodes are shown in Table 2. The polarization resistance for the sample of TNPs coated with

hydroxyapatite, copper, the drug, and chitosan has the highest value due to the presence of copper and chitosan. The sample of uncoated TNPs has the lowest value due to the lack of coating.

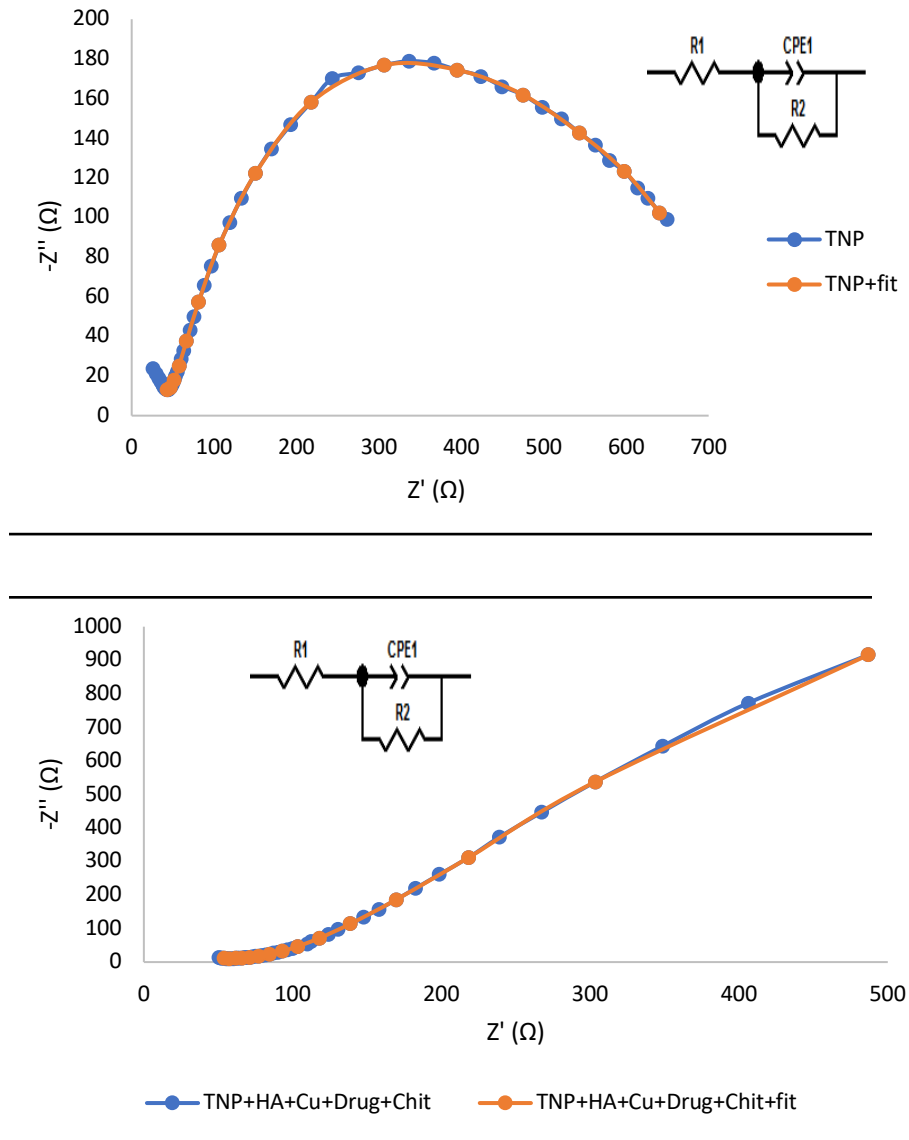


Fig. 9. Equivalent circuit of TNP, TNP/HA/Cu/Drug/Chit samples.

Table 2. Polarization resistance of TNP, TNP/HA/Drug, TNP/HA/Drug/Chit, and TNP/HA/Cu/Drug/Chit samples.

Sample	TNP/HA/Cu/Drug/Chit	TNP/HA/ Drug/Chit	TNP/HA/Drug	TNP
$R_p(\Omega)$	300,000	250,000	90,000	658.4

**Cell Viability**

Fig. 10 shows the percentage of cell viability for the samples. TNPs coated with chitosan have a higher percentage of cell viability. Among the TNPs coated with chitosan, the nanoparticles coated with hydroxyapatite, the drug, and chitosan have higher cell viability than those coated with hydroxyapatite and chitosan because the nanoparticles coated with hydroxyapatite, copper, the drug, and chitosan contain copper, which is

toxic. TNPs coated with hydroxyapatite and the drug have higher cell viability than uncoated TNPs.

**Investigation of Drug Release**

Fig. 11 shows the percentage release of sodium alendronate over 16 days for TNP/HA/Drug, TNP/HA/Drug/Chit, and TNP/HA/Cu/Drug/Chit samples. The samples of TNPs coated with hydroxyapatite 95.24%, TNPs coated with hydroxyapatite, chitosan 66.67%, and TNPs coated with hydroxyapatite, copper, chitosan 57.14%,

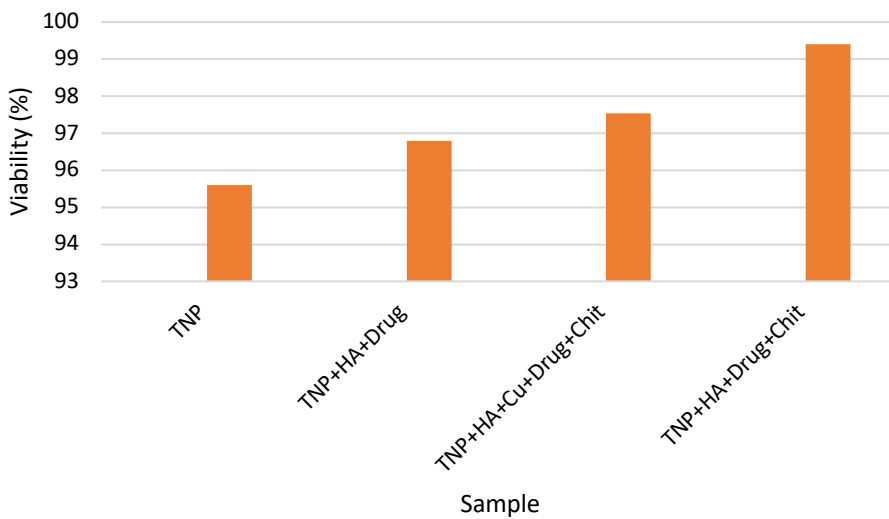


Fig. 10. Cell viability analysis of TNP, TNP/HA/Drug, TNP/HA/Drug/Chit, and TNP/HA/Cu/Drug/Chit samples.

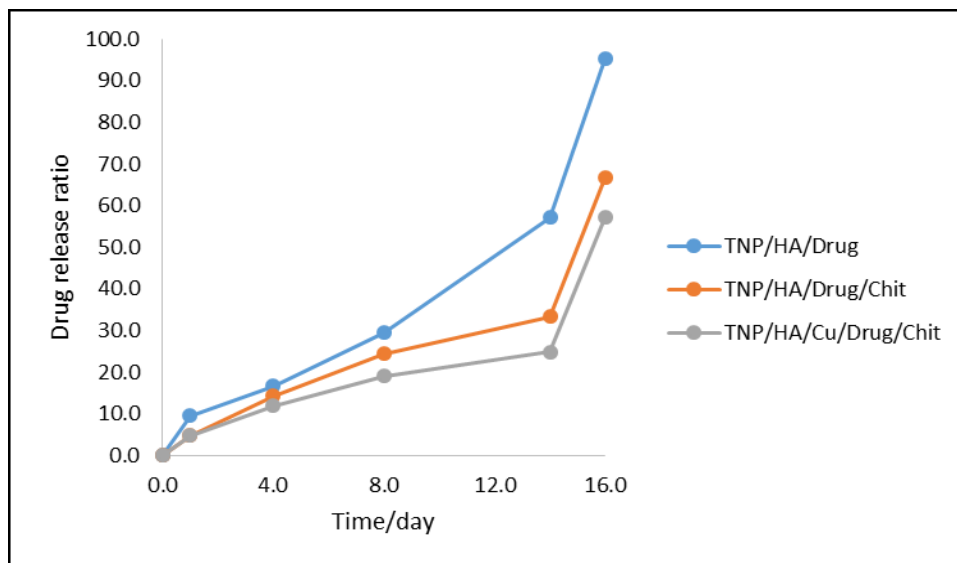


Fig. 11. The amount of drug released from coatings of TNP/HA/Drug, TNP/HA/Drug/Chit, and TNP/HA/Cu/Drug/Chit at 37 °C in the PBS for 16 days.



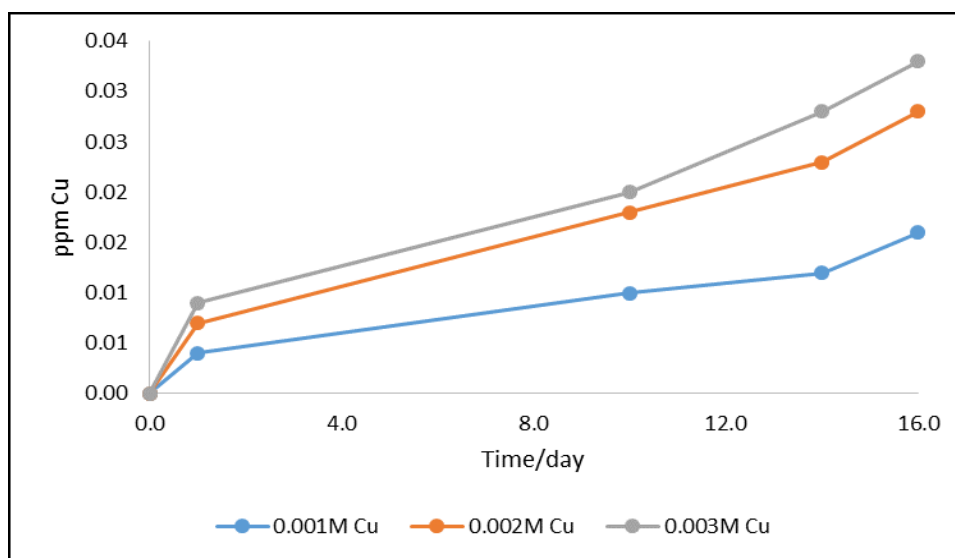


Fig. 12. The amount of Cu ion released from the coating of TNP/HA/Cu/Drug/Chit at concentrations of 0.001, 0.002, and 0.003 M copper at 37 °C in the PBS for 16 days.

and the drug were released after 16 days. The results show that for all samples, the drug release percentage was almost the same for 8 days. After 8 days, the TNP samples coated with chitosan release a lower percentage of the drug. This is due to the significant limitation of the swelling of the polymer chain, which leads to a decrease in the movement of the drug molecule and consequently a reduction in the release rate. The sample of TNPs coated with hydroxyapatite, copper, and chitosan releases a lower percentage of the drug (after 16 days) than other samples due to the increased number of layers on the surface of the nanoparticles. The TNP/HA/Cu/Drug/Chit sample was both less and more controlled due to the drug release, so it is used in implants.

#### Investigation of Copper Ion Release

Fig. 12 shows the release concentration of copper ions during 16 days for the sample of TNPs coated with hydroxyapatite, copper, drug, and chitosan with concentrations of 0.001, 0.002, and 0.003 M of copper. The concentration of copper ions released for the samples 0.001, 0.002, and 0.003 M of copper is equal to 0.016 ppm, 0.028 ppm, and 0.033 ppm, respectively. The results show that for the three samples, the percentage of copper ion release in the early days was almost the same. The concentration of copper ions released after 16 days was higher in the sample with a higher copper concentration. Copper is one of the

most important elements for essential functions in the human body, the average recommended daily intake of copper for adults is 0.9 mg per day, and the highest daily intake should not exceed 10 mg per day. In this work, the highest amount of copper released from this implant was 0.033 ppm after 16 days [44].

#### CONCLUSION

In this article, HA/Cu/Chitosan coatings on a Ti surface with anodized TiO<sub>2</sub> nanoparticles were fabricated by the electrochemical method. Drug and copper ion release percentage, cell viability percentage, corrosion resistance, and microbial analysis for modified TNPs were investigated. The percentage of drug release in TNP/HA/Drug, TNP/HA/Drug/Chit, and TNP/HA/Cu/Drug/Chit samples were compared for 16 days using a spectrophotometer, which showed that in the TNP/HA/Cu/Drug/Chit sample, due to the increased number of layers on the TNPs, the release was more controlled. The percentages of copper ion release in the TNP/HA/Cu/Drug/Chit sample with different concentrations of copper were compared for 16 days using an atomic absorption device. In the sample with a higher copper concentration, a higher percentage was released. The percentage of cell viability was compared for TNP, TNP/HA/Drug, TNP/HA/Drug/Chit, and TNP/HA/Cu/Drug/Chit samples. The TNP/HA/Drug/Chit sample had a higher percentage of cell viability

due to the absence of copper as copper is toxic. Electrochemical analyses, including polarization and impedance, were investigated for TNP, TNP/HA/Drug, TNP/HA/Drug/Chit, and TNP/HA/Cu/Drug/Chit samples. The results showed that by increasing the coatings on the surface of the implant, the resistance of the implant against corrosion increased, and the current corrosion decreased. Microbial analysis was compared for TNP, TNP/HA/Drug, TNP/HA/Drug/Chit, and TNP/HA/Cu/Drug/Chit samples. In the TNP/HA/Cu/Drug/Chit sample, the optical density value was lower than all of the samples due to the simultaneous presence of copper and chitosan, which have increased antibacterial properties. Analyses related to FESEM, EDX, XRD, and MAP were also examined.

#### ACKNOWLEDGMENT

The authors are grateful to the council of University of Kashan for supporting this work with grant no 463561-19. The authors wish to thank Yazd University Research Council for supporting this research.

#### CONFLICT OF INTEREST

The authors declare that there is no conflict of interests regarding the publication of this manuscript.

#### REFERENCES

- Huang L, Chen J, Li X, Liu H, Li J, Ren T, et al. Polymethacrylic acid encapsulated TiO<sub>2</sub> nanotubes for sustained drug release and enhanced antibacterial activities. *New J Chem.* 2019;43(4):1827-1837.
- Ammarullah MI, Afifi Y, Maula MI, Winarni TI, Tauviqirrahman M, Bayuseno AP, et al. Deformation analysis of CoCrMo-on-CoCrMo hip implant based on body mass index using 2D finite element procedure. *Journal of Physics: Conference Series.* 2022;2279(1):012004.
- Jamari J, Ammarullah MI, Santoso G, Sugiharto S, Supriyono T, Permana MS, et al. Adopted walking condition for computational simulation approach on bearing of hip joint prosthesis: review over the past 30 years. *Heliyon.* 2022;8(12):e12050-e12050.
- Jamari J, Ammarullah MI, Santoso G, Sugiharto S, Supriyono T, van der Heide E. In Silico Contact Pressure of Metal-on-Metal Total Hip Implant with Different Materials Subjected to Gait Loading. *Metals.* 2022;12(8):1241.
- Jamari J, Ammarullah MI, Saad APM, Syahrom A, Uddin M, van der Heide E, Basri H. The Effect of Bottom Profile Dimples on the Femoral Head on Wear in Metal-on-Metal Total Hip Arthroplasty. *Journal of functional biomaterials.* 2021;12(2):38.
- Prakoso AT, Basri H, Adanta D, Yani I, Ammarullah MI, Akbar I, et al. The Effect of Tortuosity on Permeability of Porous Scaffold. *Biomedicines.* 2023;11(2):427.
- Ammarullah M, Santoso G, Sugiharto S, Supriyono T, Wibowo D, Kurdi O, et al. Minimizing Risk of Failure from Ceramic-on-Ceramic Total Hip Prosthesis by Selecting Ceramic Materials Based on Tresca Stress. *Sustainability.* 2022;14(20):13413.
- Ammarullah MI, Afifi Y, Maula MI, Winarni TI, Tauviqirrahman M, Akbar I, et al. Tresca Stress Simulation of Metal-on-Metal Total Hip Arthroplasty during Normal Walking Activity. *Materials (Basel, Switzerland).* 2021;14(24):7554.
- Putra RU, Basri H, Prakoso AT, Chandra H, Ammarullah MI, Akbar I, et al. Level of Activity Changes Increases the Fatigue Life of the Porous Magnesium Scaffold, as Observed in Dynamic Immersion Tests, over Time. *Sustainability.* 2023;15(1):823.
- Jamari J, Ammarullah MI, Santoso G, Sugiharto S, Supriyono T, Prakoso AT, et al. Computational Contact Pressure Prediction of CoCrMo, SS 316L and Ti6Al4V Femoral Head against UHMWPE Acetabular Cup under Gait Cycle. *Journal of functional biomaterials.* 2022;13(2):64.
- Tauviqirrahman M, Ammarullah MI, Jamari J, Saputra E, Winarni TI, Kurniawan FD, et al. Analysis of contact pressure in a 3D model of dual-mobility hip joint prosthesis under a gait cycle. *Sci Rep.* 2023;13(1):3564-3564.
- Koopaie M, Bordbar-Khiabani A, Kolahdooz S, Darbandsari AK, Mozafari M. Advanced surface treatment techniques counteract biofilm-associated infections on dental implants. *Materials Research Express.* 2020;7(1):015417.
- Floroian L, Sima F, Florescu M, Badea M, Popescu AC, Serban N, Mihailescu IN. Double layered nanostructured composite coatings with bioactive silicate glass and polymethylmetacrylate for biomimetic implant applications. *J Electroanal Chem.* 2010;648(2):111-118.
- Harrison N, Field JR, Quondamatteo F, Curtin W, McHugh PE, Mc Donnell P. Preclinical trial of a novel surface architecture for improved primary fixation of cementless orthopaedic implants. *Clin Biomech.* 2014;29(8):861-868.
- Gebert A, Peters J, Bishop NE, Westphal F, Morlock MM. Influence of press-fit parameters on the primary stability of uncemented femoral resurfacing implants. *Medical Engineering & Physics.* 2009;31(1):160-164.
- Sakai R, Kanai N, Itoman M, Mabuchi K. Assessment of the fixation stiffness of some femoral stems of different designs. *Clin Biomech.* 2006;21(4):370-378.
- Chang J-D, Kim T-Y, Rao MB, Lee S-S, Kim I-S. Revision Total Hip Arthroplasty Using a Tapered, Press-Fit Cementless Revision Stem in Elderly Patients. *The Journal of Arthroplasty.* 2011;26(7):1045-1049.
- Götze C, Steens W, Vieth V, Poremba C, Claes L, Steinbeck J. Primary stability in cementless femoral stems: custom-made versus conventional femoral prosthesis. *Clin Biomech.* 2002;17(4):267-273.
- Chanlalit C, Fitzsimmons JS, Shukla DR, An K-N, O'Driscoll SW. Micromotion of plasma spray versus grit-blasted radial head prosthetic stem surfaces. *J Shoulder Elbow Surg.* 2011;20(5):717-722.
- Mohan L, Dennis C, Padmapriya N, Anandan C, Rajendran N. Effect of Electrolyte Temperature and Anodization Time on Formation of TiO<sub>2</sub> Nanotubes for Biomedical Applications. *Materials Today Communications.* 2020;23:101103.
- Zheng X, Sun J, Li W, Dong B, Song Y, Xu W, et al. Engineering nanotubular titania with gold nanoparticles for antibiofilm enhancement and soft tissue healing promotion. *J*

- Electroanal Chem. 2020;871:114362.
22. Salaha ZFM, Ammarullah MI, Abdullah NNA, Aziz AUA, Gan H-S, Abdullah AH, et al. Biomechanical Effects of the Porous Structure of Gyroid and Voronoi Hip Implants: A Finite Element Analysis Using an Experimentally Validated Model. *Materials* (Basel, Switzerland). 2023;16(9):3298.
  23. Ammarullah MI, Hartono R, Supriyono T, Santoso G, Sugiharto S, Permana MS. Polycrystalline Diamond as a Potential Material for the Hard-on-Hard Bearing of Total Hip Prosthesis: Von Mises Stress Analysis. *Biomedicines*. 2023;11(3):951.
  24. Santos A, Sinn Aw M, Bariana M, Kumeria T, Wang Y, Losic D. Drug-releasing implants: current progress, challenges and perspectives. *J Mater Chem B*. 2014;2(37):6157-6182.
  25. Khoshnood N, Zamaniyan A, Massoudi A. Mussel-inspired surface modification of titania nanotubes as a novel drug delivery system. *Materials Science and Engineering: C*. 2017;77:748-754.
  26. Fusi M, Maccallini E, Caruso T, Casari CS, Li Bassi A, Bottani CE, et al. Surface electronic and structural properties of nanostructured titanium oxide grown by pulsed laser deposition. *Surface Science*. 2011;605(3-4):333-340.
  27. Bariana M, Dwivedi P, Ranjitkar S, Kaidonis JA, Losic D, Anderson PJ. Biological response of human suture mesenchymal cells to Titania nanotube-based implants for advanced craniostylosis therapy. *Colloids Surf B Biointerfaces*. 2017;150:59-67.
  28. Feng W, Geng Z, Li Z, Cui Z, Zhu S, Liang Y, et al. Controlled release behaviour and antibacterial effects of antibiotic-loaded titania nanotubes. *Materials Science and Engineering: C*. 2016;62:105-112.
  29. Kumeria T, Mon H, Aw MS, Gulati K, Santos A, Griesser HJ, Losic D. Advanced biopolymer-coated drug-releasing titania nanotubes (TNTs) implants with simultaneously enhanced osteoblast adhesion and antibacterial properties. *Colloids Surf B Biointerfaces*. 2015;130:255-263.
  30. Xu J, Xu N, Zhou T, Xiao X, Gao B, Fu J, Zhang T. Polydopamine coatings embedded with silver nanoparticles on nanostructured titania for long-lasting antibacterial effect. *Surf Coat Technol*. 2017;320:608-613.
  31. Liu X, Tian A, You J, Zhang H, Wu L, Bai X, et al. Antibacterial abilities and biocompatibilities of Ti-Ag alloys with nanotubular coatings. *International journal of nanomedicine*. 2016;11:5743-5755.
  32. Xi T, Shahzad MB, Xu D, Sun Z, Zhao J, Yang C, et al. Effect of copper addition on mechanical properties, corrosion resistance and antibacterial property of 316L stainless steel. *Materials Science and Engineering: C*. 2017;71:1079-1085.
  33. Hadidi M, Bigham A, Saebnoori E, Hassanzadeh-Tabrizi SA, Rahmati S, Alizadeh ZM, et al. Electrophoretic-deposited hydroxyapatite-copper nanocomposite as an antibacterial coating for biomedical applications. *Surf Coat Technol*. 2017;321:171-179.
  34. Çalışkan N, Bayram C, Erdal E, Karahaliloğlu Z, Denkbaş EB. Titania nanotubes with adjustable dimensions for drug reservoir sites and enhanced cell adhesion. *Materials Science and Engineering: C*. 2014;35:100-105.
  35. Zhang K, Zhu Y, Liu X, Cui Z, XianjinYang, Yeung KWK, et al. Sr/ZnO doped titania nanotube array: An effective surface system with excellent osteoinductivity and self-antibacterial activity. *Materials & Design*. 2017;130:403-412.
  36. van Hengel IAJ, Tierolf MWAM, Fratila-Apachitei LE, Apachitei I, Zadpoor AA. Antibacterial Titanium Implants Biofunctionalized by Plasma Electrolytic Oxidation with Silver, Zinc, and Copper: A Systematic Review. *Int J Mol Sci*. 2021;22(7):3800.
  37. Felt O, Buri P, Gurny R. Chitosan: A Unique Polysaccharide for Drug Delivery. *Drug Development and Industrial Pharmacy*. 1998;24(11):979-993.
  38. Hamdi DA, Jiang Z-T, No K, Rahman MM, Lee P-C, Truc LNT, et al. Biocompatibility study of multi-layered hydroxyapatite coatings synthesized on Ti-6Al-4V alloys by RF magnetron sputtering for prosthetic-orthopaedic implant applications. *Appl Surf Sci*. 2019;463:292-299.
  39. Kaushik N, Nhat Nguyen L, Kim JH, Choi EH, Kumar Kaushik N. Strategies for Using Polydopamine to Induce Biomaterialization of Hydroxyapatite on Implant Materials for Bone Tissue Engineering. *Int J Mol Sci*. 2020;21(18):6544.
  40. Govindharajulu JP, Chen X, Li Y, Rodriguez-Cabello JC, Battacharya M, Aparicio C. Chitosan-Recombinamer Layer-by-Layer Coatings for Multifunctional Implants. *Int J Mol Sci*. 2017;18(2):369.
  41. Bordbar-Khiabani A, Yarmand B, Mozafari M. Functional PEO layers on magnesium alloys: innovative polymer-free drug-eluting stents. *Surface Innovations*. 2018;6(4-5):237-243.
  42. Bordbar-Khiabani A, Yarmand B, Sharifi-Asl S, Mozafari M. Improved corrosion performance of biodegradable magnesium in simulated inflammatory condition via drug-loaded plasma electrolytic oxidation coatings. *Materials Chemistry and Physics*. 2020;239:122003.
  43. Tuomi JT, Björkstrand RV, Pernu ML, Salmi MVJ, Huotilainen EI, Wolff JEH, et al. In vitro cytotoxicity and surface topography evaluation of additive manufacturing titanium implant materials. *J Mater Sci Mater Med*. 2017;28(3).
  44. Yang H-L, Zou L, Juaim AN, Ma C-X, Zhu M-Z, Xu F, et al. Copper release and ROS in antibacterial activity of Ti-Cu alloys against implant-associated infection. *Rare Metals*. 2023;42(6):2007-2019.